5846–5862 *Nucleic Acids Research, 2014, Vol. 42, No. 9* *Published online 01 April 2014*
doi: 10.1093/nar/gku237

Human MUS81-EME2 can cleave a variety of DNA structures including intact Holliday junction and nicked duplex

Tamir Amangyeld, Yong-Keol Shin, Miju Lee, Buki Kwon and Yeon-Soo Seo*

Department of Biological Sciences, Korea Advanced Institute of Science and Technology, Daejeon 305-701, Korea

Received August 21, 2013; Revised March 6, 2014; Accepted March 7, 2014

ABSTRACT

MUS81 shares a high-degree homology with the catalytic XPF subunit of the XPF–ERCC1 endonuclease complex. It is catalytically active only when complexed with the regulatory subunits Mms4 or Eme1 in budding and fission yeasts, respectively, and EME1 or EME2 in humans. Although Mus81 complexes are implicated in the resolution of recombination intermediates *in vivo*, recombinant yeast Mus81-Mms4 and human MUS81-EME1 isolated from *Escherichia coli* fail to cleave intact Holliday junctions (HJs) *in vitro*. In this study, we show that human recombinant MUS81-EME2 isolated from *E. coli* cleaves HJs relatively efficiently, compared to MUS81-EME1. Furthermore, MUS81-EME2 catalyzed cleavage of nicked and gapped duplex deoxyribonucleic acids (DNAs), generating double-strand breaks. The presence of a 5′ phosphate terminus at nicks and gaps rendered DNA significantly less susceptible to the cleavage by MUS81-EME2 than its absence, raising the possibility that this activity could play a role in channeling damaged DNA duplexes that are not readily repaired into the recombinational repair pathways. Significant differences in substrate specificity observed with unmodified forms of MUS81-EME1 and MUS81-EME2 suggest that they play related but non-overlapping roles in DNA transactions.

INTRODUCTION

In human cells, more than six billion base pairs of deoxyribonucleic acid (DNA) must be replicated and packaged into chromosomes every cell division cycle. Completion of chromosomal DNA replication requires successful propagation of all replication forks (RFs). During DNA replication, RFs are likely to encounter numerous replication blockage sites caused by DNA damage or tightly bound proteins, interfering with the faithful duplication of genomic DNA (1,2). In order to cope with potential risks of genome instability, eukaryotic cells have developed several mechanisms to repair impaired RFs. When RFs encounter lesions in template DNA, RFs will be stalled or eventually broken. Such RF-associated double-strand breaks (DSBs) can be repaired by recombinational repair pathways (3,4). Alternatively, RFs can form chicken-foot structures that are similar to Holliday junctions (HJs) by annealing regressed leading and lagging strands upon blockage of their progression due to lesions (5,6). Such structures need to be resolved or reversed through junction migration prior to the re-establishment of functional RFs. The enzymatic activities normally required for resolution of recombination intermediates can also be used to restart impaired RFs. The resolution of four-way arm structures can be achieved by HJ resolvases, structure-selective endonucleases that introduce paired cleavages in the two opposing strands at the branch point of HJs (7). Reversal of the regressed RFs can be achieved by a specific set of DNA helicases that include a member of the RecQ helicases (8).

HJ resolvases are universal, being found in a wide range of organisms such as bacteriophages, eubacteria, archaea, to eukaryotic viruses (7,9). They can be divided into two categories based on their *in vitro* substrate specificity. The first group, which includes bacterial RuvC, bacteriophage RusA, archaeal Hjc and mitochondrial CCE1 proteins, has a stringent preference for HJs (10–12). In contrast, the second group including bacteriophage T4 endo VII and T7 endo I enzymes displays reduced specificity; they are shown to cleave HJ as well as other branched DNA structures (7,9).

Recently, two novel HJ resolvases that cleave HJs symmetrically were identified in humans; GEN1 (13,14) and SLX1-SLX4 (15,16). GEN1 acts preferentially on 5′-flaps, RFs and HJ substrates and has the ability to dimerize on HJs and introduce the symmetrical dual incisions (14). SLX1-SLX4 plays an important role in the repair of DSBs and interstrand crosslinks, and its ortholog in *Drosophila*, MUS312, is critical for meiotic crossover formation (17). Another human endonuclease that acts as an HJ resolvase is MUS81-EME1, a member of the XPF family of structure-selective endonucleases (18). Human MUS81 forms stable

*To whom correspondence should be addressed. Tel: +82 42 350 2637; Fax: +82 42 350 2610; E-mail: yeonsooseo@kaist.ac.kr

complexes with either EME1 or EME2. EME2 was identified by its sequence similarity to EME1 and showed 44% identity with EME1, with the highest homology located at the C-terminal region (19). The human MUS81–EME2 complex was shown to process 3′-flap (3′F) substrates like human MUS81-EME1 (20). In parallel with the enzymatic cleavage of HJ structures, eukaryotic cells have a redundant pathway that does not involve a structure-specific nuclease. For example, double HJs arising during repair of impaired RFs can be resolved by the Sgs1–Top3–Rmi1 complex in *Saccharomyces cerevisiae* and the BLM–Top IIIα–RMI1–RMI2 complex in humans. This type of resolution, termed dissolution, does not rely on conventional HJ resolvase activity and always gives rise to non-crossover products (21).

Substantial data indicate that the structure-selective endonuclease activity of Mus81 is important for the repair of stalled RFs in somatic cells. In *S. cerevisiae*, *mus81* mutants were sensitive to DNA-damaging agents including ultraviolet (UV) radiation, hydroxyurea, methylmethane sulfonate or camptothecin that cause RFs to stall or collapse (22–25). It was reported that the Mus81 protein physically interacted with Cds1, a DNA damage checkpoint kinase in *Schizosaccharomyces pombe*, and with Rad54, a recombination protein in *S. cerevisiae* (22,23). In human cells, MUS81 is mainly localized in nuclei and recruited to UV-induced damage sites in S-phase cells (26). These observations are in keeping with an *in vivo* role of Mus81 in resolving abnormal structures including stalled RFs as suggested (27).

It was shown that human recombinant MUS81-EME1 efficiently cleaved branched DNA substrates such as 3′F, RF and nicked HJ (nHJ), but poorly (∼75-fold less compared to nHJ) cleaved intact HJ (iHJ) structures (19). The presence of a mobile core junction at iHJ substantially (>10-fold) increased the rate of cleavage. The strong preference of nHJ over iHJ structure is characteristic of all known Mus81 complexes including the recombinant *S. cerevisiae* Mus81–Mms4 and *S. pombe* Mus81–Eme1 complexes (24,28–30). The low rate of cleavage of iHJ could be attributed to a nick-and-counternick mechanism, in which an initial nicking event at the junction is slow, but the subsequent nicking event is rapid (10). MUS81-EME1 also interacts with the human SLX1–SLX4 complex, raising the possibility that these nucleases cooperate in processing HJs (15,16). In *S. pombe*, the phenotypes of the *mus81* or *eme1* (*mms4* in *S. cerevisiae*) mutations, including sensitivity to DNA damaging agents and synthetic lethality with *rqh1* (*sgs1* in *S. cerevisiae*) mutations, are suppressed by the overexpression of RusA, a bacterial HJ resolvase (24). In humans immunoprecipitates of MUS81 complexes derived from HeLa cells were shown to cleave iHJ (31). These findings raise the possibility that an unidentified factor associated with the MUS81 complex is required for the resolution of iHJs in eukaryotes. The discrepancy in the ability to cleave iHJ between the highly purified recombinant and immunoprecipitated (or partially purified) endogenous Mus81 complexes requires clarification as addressed in part here.

In this report, we investigated the enzymatic properties of human MUS81-EME1 and MUS81-EME2 in order to give insight into their functional roles *in vivo*. We found that the recombinant MUS81–EME2 complex cleaved iHJ substrate *in vitro* in contrast to MUS81-EME1, indicating that the regulatory subunit affects the substrate specificity. In addition, we discovered that MUS81-EME2 cleaved nicked duplex (nDS) and gapped duplex (gDS) DNAs to form DSBs. Cleavage of nDS or gDS was significantly decreased by the presence of 5′ phosphate ends at nicks or gaps. Duplex DNAs with unligatable nicks were cleaved preferentially by the human MUS81–EME2 complex. Thus, this enzymatic activity could contribute to the repair of some types of DNA damages by facilitating DSB-initiated homologous recombination. Our findings indicate that MUS81-EME2 plays a more versatile and dominant role, although not entirely distinct from, than MUS81-EME1 in dealing with various aberrant structures that arise during DNA transactions.

MATERIALS AND METHODS

Chemicals, nucleotides, enzymes and DNAs

The oligonucleotides used in this study were synthesized commercially by Bioneer and Genotech (Daejeon, Korea). Oligonucleotides longer than 30 nucleotides (nt) were gel-purified prior to use. The following proteins: Taq DNA polymerases, restriction endonucleases, T4 DNA ligase and polynucleotide kinase were purchased from Enzynomics (Daejeon, Korea). Nucleoside triphosphates were obtained from Sigma-Aldrich (St. Louis, MO, USA). [γ-^{32}P] ATP (>5000 Ci/mmol) was purchased from IZOTOP (Budapest, Hungary). Isopropyl β-D-1-thiogalactopyranoside (IPTG) was from ElpisBiotech, Inc. (Daejeon, Korea) and imidazole (IDZ) was from Acros Organics (Geel, Belgium). The expression vectors (pET21d-MUS81/His-EME1 and pET21d-MUS81/His-EME2) used to prepare the MUS81–EME1/EME2 complexes were kindly provided by Dr Stephen C. West (London Research Institute, UK). In expression vectors, 'His' before the name of proteins indicates that hexahistidine tags were fused to the N-terminus of the expressed proteins.

Preparation of DNA substrates

The oligonucleotides (and sequences) used for substrate preparations are listed in Table 1. Schematic representation of DNA substrates and oligonucleotides used are shown in each figure. nDS or gDS DNA substrates were prepared as follows: one of the indicated oligonucleotides (20 pmol) was 5′-labeled with 3.3 pmol of [γ-^{32}P] ATP and polynucleotide kinase according to the manufacturer's protocol. Labeled oligonucleotides were then annealed with the other two oligonucleotides at a molar ratio of 1:1:1 in 150-mM NaCl in TE buffer [10-mM Tris-HCl/pH8.0, 1-mM ethylenediaminetetraacetic acid (EDTA)] using a polymerase chain reaction (PCR) machine (95°C: 15 min; 65°C: 30 min; and −0.5°C /8 min to 25°C). For preparation of 3′F substrates, one of the indicated oligonucleotides was labeled as described above and annealed with the other two oligonucleotides at a molar ratio of 1.5 (the labeled one):2 (the other two). To prepare RF, regressed RFs, iHJ and nHJ substrates, one of the indicated oligonucleotides was labeled and annealed with the other oligonucleotides at the same molar ratio. The resulting substrates were gel-purified prior to use.

Table 1. Oligonucleotide sequences used in this study

No.	Nucleotide sequences (length in nt)	Name
1.	CGAACAATTCAGCGGCTTTAACCGGACGCTCGACGCCATTAATAATGTTTTC(52)	729
2.	CGCATCCTATCAGTTCGTATGCAGTGTCCGGTTAAAGCCGCTGAATTGTTCG(52)	Anti729-1
3.	CCGTTAGCAGTTCGCCTTGTGCCTAACTGCATACGAACTGATAGGATGCG(50)	Anti 729-2+5TB
4.	GAAAACATTATTAATGGCGTCGAGCTAGGCACAAGGCGAACTGCTAACGG(50)	5TY-1
5.	ACTGCATACGAACTGATAGGATGCG(25)	Anti 729-2
6.	CCGTTAGCAGTTCGCCTTGTGCCTA(25)	5TB
7.	GAAACATTATTAATGGCGTCGAGC(25)	Anti 729-3
8.	GCTCGACGCCATTAATAATGTTTTC (25)	729-no flap

Purification of recombinant MUS81-EME2

The recombinant human MUS81–EME2 complex was purified as previously described (20,32) with the following modifications. The pET21d-MUS81/His-EME2 plasmid was transformed into *Escherichia coli* BL21-Codon plus (DE3) RIL (Stratagene) and cells (2 l) were grown at 30°C until an A_{600} value of 1.0. Cells were then induced with 0.1-mM IPTG (final concentration) for 3 h and harvested by centrifugation. The cell pellet was resuspended in 100 ml of buffer P_{300} [50-mM sodium phosphate/pH 7.0, 300-mM NaCl, 10% glycerol, 0.1% NP-40, 1-mM phenylmethlysulfonyl fluoride and 0.1-mM benzamidine]. The subscript number in P_{300} indicates the concentration of NaCl in mM. Cells were then lysed using a Vibra cell sonicator (Sonics & Materials, Inc., CT, USA). After sonication, the cell extract was centrifuged for 50 min at 18 000 rpm and the supernatant loaded directly onto a 10-ml phosphocellulose column (Φ 1.5 × 5.7 cm) pre-equilibrated with buffer P_{300}. Bound proteins were eluted stepwise using buffers P_{300}, P_{700} and P_{1000} (50 ml each). Fractions eluting with buffer P_{700} contained endonuclease activity detected with nHJ substrates. Peak endonuclease fractions were pooled and mixed with 3 ml of Ni^{2+}-NTA (nickel-nitrilotriacetic acid) agarose beads (Qiagen; Valencia, CA, USA). The agarose beads were collected and washed extensively with buffer P_{300}. Proteins were then eluted successively with buffer P_{300} plus 50, 70 and 300-mM IDZ. Fractions from each elution were assayed for endonuclease activity. The peak activity fractions were pooled and loaded directly onto a 1-ml heparin column pre-equilibrated in buffer P_{300}. Proteins bound to the heparin beads were eluted using a 35-ml linear gradient of buffer P containing 0.3–1.5-M NaCl, and the resulting fractions analyzed for endonuclease activity and protein. The eluted fractions containing the least contaminant proteins (eluting between 0.7 and 0.8 M NaCl) were collected, and an aliquot (250 μl) was subjected to glycerol gradient sedimentation (5 ml, 15–35% glycerol in buffer P_{300}) at 55 000 rpm for 24 h in a SW55 Ti rotor (Beckman). Fractions (∼250 μl each) were collected from the bottom of the tube and stored as aliquots at −80°C until use. Protein levels were measured using a Bio-Rad protein assay kit with bovine serum albumin (BSA) as standard during each purification step. For an accurate comparison of specific activities of the MUS81 complexes, we performed quantitative densitometric determination of the concentrations of each complex with BSA as control. MUS81 complexes are heterodimeric and therefore the level of the complex used in the experiments described represents moles of heterodimers.

Nuclease assay

Standard nuclease assays were performed in reaction mixtures (20 μl) containing 25-mM Tris-HCl/pH 8.0, 1-mM $MgCl_2$, 0.2-mM dithiothreitol (DTT), 0.1-mg/ml BSA, 0.1% NP-40, 5% glycerol, 30-mM NaCl and 15 fmol of DNA substrate. MUS81-EME2 was diluted in buffer T_{300} (50-mM Tris-HCl/pH 7.5, 300-mM NaCl, 1-mM DTT, 0.1-mg/ml BSA and 25% glycerol) prior to its addition to reaction mixtures. Reaction mixtures were incubated at 37°C for 30 min, and reactions terminated with 4 μl of 6X stop solution [60-mM EDTA/pH 8.0, 40% sucrose, 1.2% sodium dodecyl sulphate (SDS), 0.05% bromophenol blue and 0.05% xylene cyanol]. Products were subjected to electrophoresis through either 10% non-denaturing (40 min, 130 V) or 15% denaturing (plus 7-M urea; 90 min, 30 W) polyacrylamide gel in 1X TBE (89-mM Tris-base, 89-mM boric acid and 2-mM EDTA). The gels were dried on DEAE-cellulose paper and autoradiographed. Labeled DNA products were quantified using a phosphor imager (BAS-1500, Fujifilm). When two products were formed, the amounts of both slow-migrating (large) and fast-migrating (small) products were determined and are indicated in each figure. Error bars were included when experiments were carried out more than three times, e.g. in the graphs of Figures 6B and 7B. For the rest of the graphs shown, we used the most representative one.

RESULTS

Purification of the recombinant MUS81–EME2 complex

In order to gain insight into the physiological role of the two human MUS81 complexes, we decided to compare biochemical properties of recombinant human MUS81-EME1 and MUS81-EME2 isolated from *E. coli*. For this purpose, we expressed and purified recombinant human MUS81–EME1/EME2 complexes to near homogeneity. While purifying the complexes, we noted that MUS81-EME2 cleaved iHJ structure in contrast to MUS81-EME1 (data not shown; see below). This finding prompted us to purify the MUS81–EME2 complex more rigorously using two additional purification steps; heparin-column chromatography and glycerol gradient sedimentation. The active fractions obtained with 300-mM IDZ from the Ni^{2+}-NTA affinity column were pooled (Fraction III; Figure 1A) and loaded

onto a heparin column. The column was then eluted with a linear gradient of 0.3–1.5-M NaCl (Figure 1A). The resulting fractions were analyzed for both MUS81-EME2 proteins and iHJ-cleavage activity. We found that HJ-cleavage activity copurified with the MUS81–EME2 complex (data not shown). The peak of this activity eluted between 0.7 and 0.8 M of NaCl (Fraction IV; Figure 1A), however, still contained two additional polypeptides as major contaminants (Figure 1B, lane 1). In order to verify that MUS81-EME2 was responsible for the cleavage of iHJ as well as to remove the two contaminating polypeptides, an aliquot (250 μl) of Fraction IV was subjected to 15–35% glycerol gradient sedimentation. As shown in Figure 1B, the MUS81–EME2 complex was well separated from the two contaminated polypeptides. Like all the other Mus81 complexes, the two subunits in the complex displayed a 1:1 stoichiometric ratio in densitometric analyses with BSA as control.

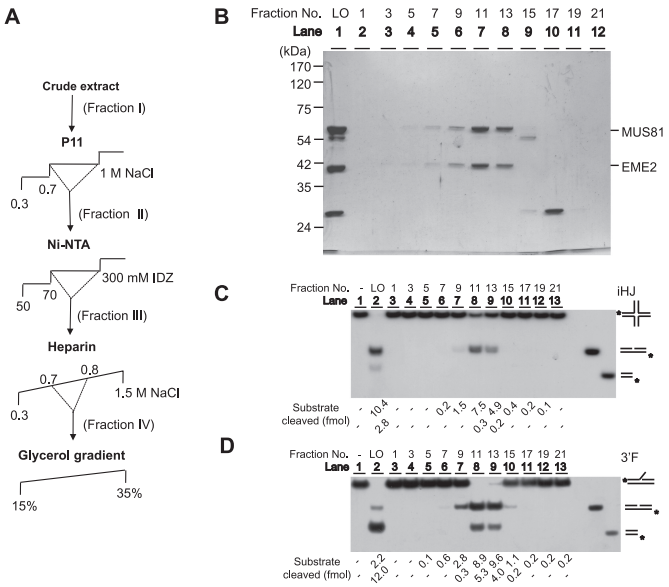

Figure 1. Purification of the recombinant human MUS81-EME2 complex from *E. coli* extracts that contains intrinsic endonuclease activity which can cleave intact Holliday junction (iHJ). (**A**) The purification scheme used to purify the recombinant human MUS81-EME2 complex. The recombinant human MUS81-EME2 was expressed in *E. coli* and purified using the same procedure as reported (20,32), but modified by the introduction of two additional purification steps (see text for details). P11, Ni^{2+}-NTA and heparin indicate phosphocellulose, Ni^{2+}-NTA affinity and heparin column chromatography, respectively. IDZ, imidazole. Glycerol gradient indicates the final purification procedure using glycerol gradient sedimentation. Fraction I is the crude extract prepared from *E. coli* carrying the bicistronic vector pET21d-MUS81/His-EME2 (20), and other fractions from each step are as indicated. (**B**) An aliquot (250 μl) of Fraction IV from heparin column chromatography was subjected to glycerol gradient sedimentation and the resulting fractions were analyzed in a 10% SDS-PAGE and the gel was stained with Coomassie Brilliant Blue R-250. The sizes of molecular mass markers are indicated in kDa. The positions of MUS81 and EME2 are as indicated. LO, load-on. (**C**) and (**D**) A fixed amount (15 fmol) of intact iHJ [panel (C)] and 3′ flap (3′F) [panel (D)] substrates was incubated with 0.02 μl (1 μl of 50-fold dilution) of the indicated glycerol gradient fractions of MUS81-EME2 at 37°C for 30 min. The schematic structures of the substrate and marker DNA are shown at the right side of the gel. The DNA substrates used were prepared as described in the Materials and Methods section. Asterisks indicate the position of the 5′-^{32}P label. Two marker DNAs (2-nt gapped 50-bp linear and 25-bp linear duplex DNA) were used as indicated to monitor the migration of DNA products. Reaction products were subjected to 10% polyacrylamide gel electrophoresis (PAGE) in 1X TBE at 130 V. The amount of cleavage product formed is indicated at the bottom of the gel. LO, load-on (Fraction IV in Figure 1A).

Endonuclease activities of MUS81–EME2 complex

We first checked for endonuclease activities across the glycerol gradient fractions using the iHJ substrate (Figure 1C). When 15 fmol of the iHJ substrate was incubated with 0.02 μl (1 μl of 50-fold diluted fraction) of every other fraction in the standard reaction condition, the amount of products formed was proportional to the level of MUS81–EME2 complex present in the glycerol gradient fractions, indicating that HJ-cleavage activity is intrinsic to the MUS81–EME2 complex (Figure 1C). We noticed that the gDS products (the first cleavage products from HJ) were further cleaved to smaller DNA upon prolonged incubation (data not shown; see below) or by high enzyme levels such as the load-on control (Figure 1C, lane 2).

The same experiment was repeated with a 3′F substrate, the most efficient substrate for all known MUS81 endonucleases (Figure 1D). As expected, the cleavage efficiency of the 3′F substrate was significantly higher than that of the iHJ substrate. The addition of 0.02 μl of glycerol fractions 11 and 13 in reactions resulted in saturation for the cleavage of the 3′F substrate (Figure 1D, lanes 8 and 9), while leading to the quantitative cleavage of ∼50% (7.5 fmol) and ∼30% (4.9 fmol), respectively, of the iHJ substrate used (Figure 1C, lanes 8 and 9). Additional cleavage products were markedly increased with the 3′F substrate (compare lanes 2 and 7–9 in Figure 1C and D). The sum of the two products formed was proportional to the level of proteins in the fractions, indicating that MUS81-EME2 was responsible for this activity as well. To verify that gDS DNAs were cleaved by MUS81-EME2, nDS or gDS substrates were prepared and analyzed in a similar experiment. We noticed that the cleavage activity with the two substrates was also intrinsically associated with human MUS81-EME2 (data not shown; see below). These results demonstrate that the recombinant human MUS81–EME2 complex is able to cleave iHJ and nDS or gDS substrates, while human MUS81–EME1 complex or other yeast Mus81 complexes (*S. cerevisiae* Mus81-Mms4 or *S. pombe* Mus81-Eme1) are not (10,19,24).

In order to more clearly define substrate specificity of MUS81-EME2, we carried out kinetic analyses to determine K_M and V_{max} of MUS81-EME2 for 3′F and iHJ substrates. As summarized in Table 2, MUS81-EME2 showed a 2-fold higher V_{max} value with 3′F than with iHJ, but displays a lower K_M for iHJ. The values k_{cat} and catalytic efficiency (K_M/k_{cat}) of MUS81-EME2 for 3′F were 10- and 5-fold higher, respectively, than those for iHJ (Table 2). These results demonstrate that MUS81-EME2 is able to utilize the 3′F markedly more efficiently over the HJ substrate. In this regard, human MUS81-EME2 retains a substrate preference similar to that observed previously with yeast Mus81-Mms4 (30).

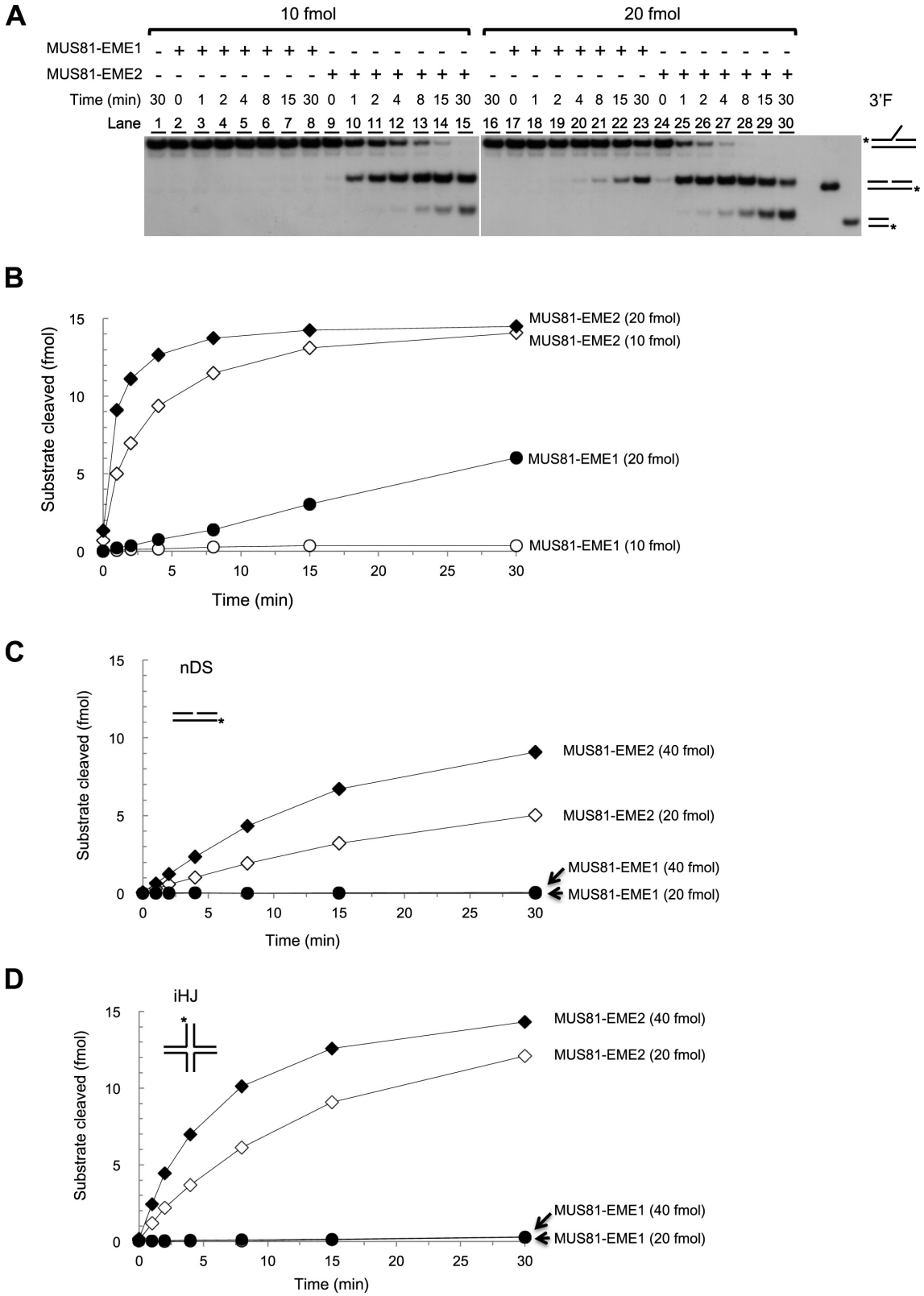

Figure 2. Comparison of endonuclease activities of human MUS81-EME1 and MUS81-EME2 complexes. Standard endonuclease assays were performed with 15 fmol of 3′F (**A**) and (**B**), nDS (**C**) and iHJ (**D**) substrates in the presence of varying amounts (10, 20 or 40 fmol) of MUS81-EME1 and MUS81-EME2 complexes. Assays were performed at 37°C and reactions were stopped at the indicated time points (1, 2, 4, 8, 15 and 30 min). Addition or omission of MUS81-EME2 is indicated by '+' or '−', respectively. DNA substrates and the marker DNAs are shown at the right side of the gel. The amount of cleavage product formed is indicated at the bottom of the gel. Asterisks indicate the position of the 5′-^{32}P label. (B)–(D) The amount of cleavage products was plotted against the time of incubation.

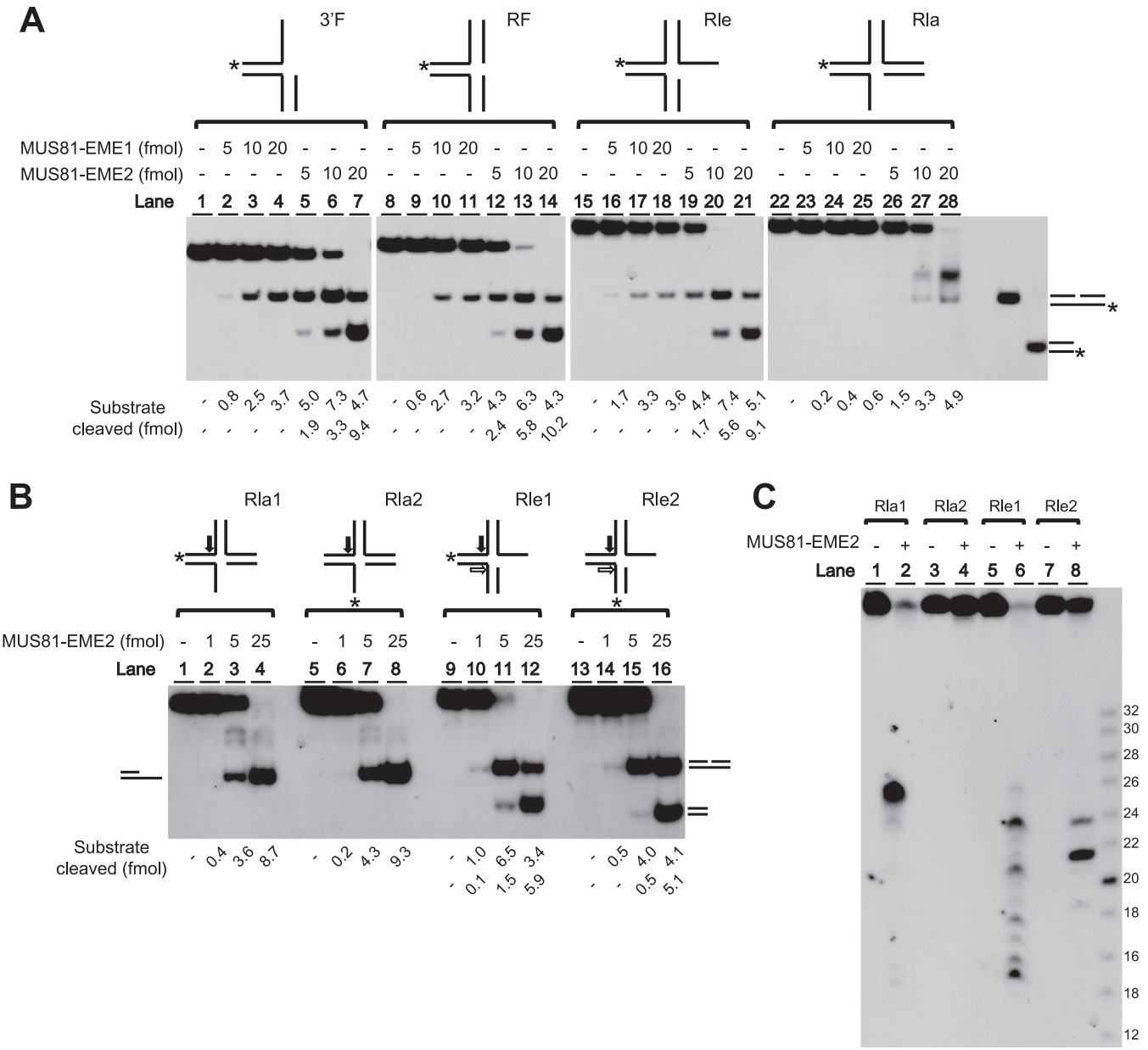

Figure 3. Human MUS81-EME2 processed different RF structures. (**A**) Standard endonuclease assays were performed with 15 fmol of 3′F, RF, Rle and Rla substrates in the presence of increasing amount (5, 10 and 20 fmol) of MUS81 complexes. The substrates used are indicated at the top of the gel. Asterisks indicate the position of the 5′-^{32}P label. Reaction mixtures were incubated at 37°C for 30 min. (**B**) The same reaction as in panel (A) was repeated with differently labeled Rla and Rle substrates. Rla and Rle substrates (10 fmol) were incubated with increasing amounts (1, 5 and 25 fmol) of MUS81-EME2 at 37°C for 60 min. Omission of protein is indicated by '−'. The structures of the DNA substrates used are shown at the top of the gel. Shown at the left and right of the gel are the structures of cleavage products. The amount of cleavage products is indicated at the bottom of the gel. The primary and secondary cleavage sites are indicated by the solid and open arrows, respectively, for each substrate used. (**C**) The reaction mixtures incubated with 25 fmol of MUS81-EME2 and each substrate as indicated above the gel were stopped by the addition of 2X stop solution (95% formamide, 20-mM EDTA, 0.1% bromophenol blue and 0.1% xylene cyanol) after 60 min of incubation at 37°C, and cleavage products were subjected to 15% denaturing PAGE containing 7-M urea. The molecular size markers are synthetic oligonucleotides labeled at their 5′ ends, and their size (nt) is indicated.

Optimal reaction conditions for MUS81–EME2 complex

Prior to characterize the enzymatic activities of the human MUS81-EME2, we determined the optimal reaction conditions for this enzyme. We examined the influence of salts, divalent metal ions and pH on its enzymatic activity. With 3′F and iHJ substrates (15 fmol each), the optimal activity was detected from 30 to 50-mM NaCl with pH between 7.5 and 8.5 (data not shown). The influences of temperature and time of incubation on the endonuclease activity were also examined; MUS81-EME2 was most stable at 30°C than 37°C, but remained active at 37°C up to 30 min of incubation (data not shown). Mg^{2+} and Mn^{2+} supported the cleavage of iHJ by MUS81-EME2, though their optimal concentrations differed, ranging from 0.5 to 2 mM and from 0.25 to 0.5 mM, respectively (Table 3). Co^{2+} supported

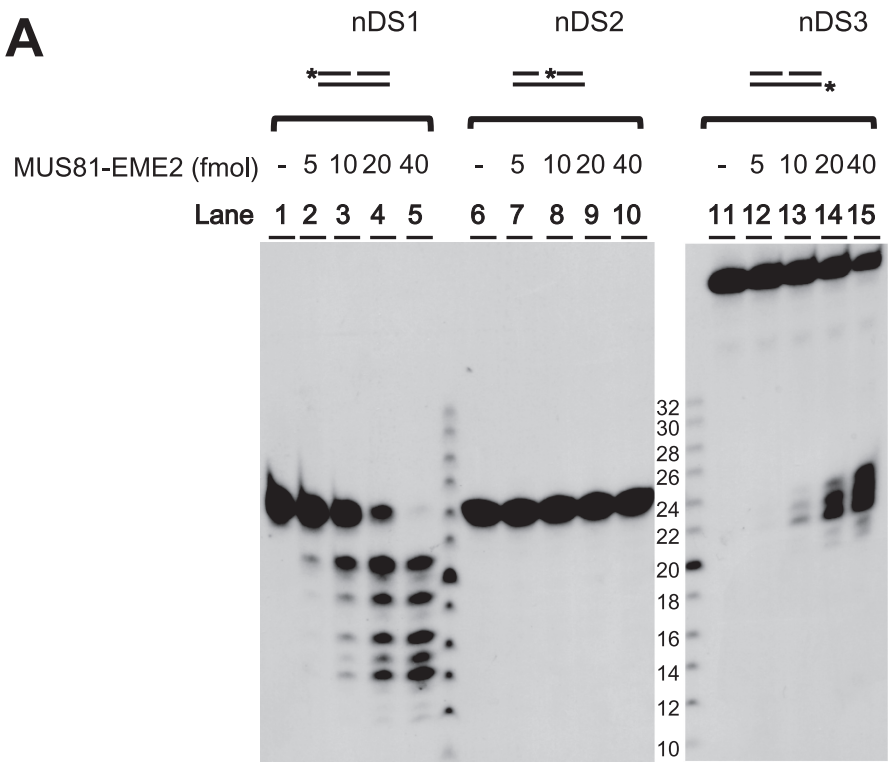

Figure 4. Analysis of cleavage of each strand in an nDS DNA substrate by human MUS81-EME2. (**A**) Reaction mixtures containing 15 fmol of one of the nDS (nDS1, nDS2 and nDS3) substrates and increasing amounts (5, 10, 20 and 40 fmol) of MUS81-EME2 were incubated at 37°C for 30 min. The cleavage products were subjected to 15% denaturing PAGE. The molecular mass markers are as described in Figure 4C. Asterisks indicate the position of the ^{32}P-label.(**B**) The cleavage sites of MUS81-EME2 on the nDS substrate are indicated by arrows; longer arrows indicate more preferred cleavage sites.

the cleavage of iHJ substrates only at low levels (0.25 mM), but less efficiently compared to Mn^{2+} and Mg^{2+}, while Ca^{2+} and Zn^{2+} were inactive (Table 3). We noted that MUS81-EME2 cleaved the 3′F and iHJ substrates somewhat non-specifically in the presence of Mn^{2+}, in keeping with a previous report for other Mus81 enzymes (33). Based on these finding, the standard reaction mixtures and reaction conditions were determined as described in the Materials and Methods section and used in all subsequent studies.

Comparison of substrate specificity of MUS81-EME1 and MUS81-EME2

Compared to the well-studied Mus81 complexes (including *S. cerevisiae* Mus81-Mms4, *S. pombe* Mus81-Eme1 and human MUS81-EME1), human MUS81-EME2 has been poorly characterized. Therefore, we examined the endonuclease activities of the two human MUS81 complexes isolated from *E. coli* to better understand their biochemical properties. To this end, we first examined their substrate specificities using different DNA substrates. In the presence of low levels (10 fmol) of enzyme, the 3′F substrate was efficiently cleaved by MUS81-EME2, while much less so by MUS81-EME1 (Figure 2A, compare lanes 2–8 and 9–15; Figure 2B) (20). MUS81-EME2 cleaved the 3′F substrate at least >50-fold faster (8.3×10^{-3} s^{-} versus 1.4×10^{-4} s^{-}) than MUS81-EME1 (Figure 2B). In keeping with the above results (Figure 1D), MUS81-EME2 produced two cleavage products (Figure 2A, lanes 9–15 and 24–30), while MUS81-EME1 formed only gDS products (Figure 2A, lanes 17–28). More marked substrate specificity was observed with

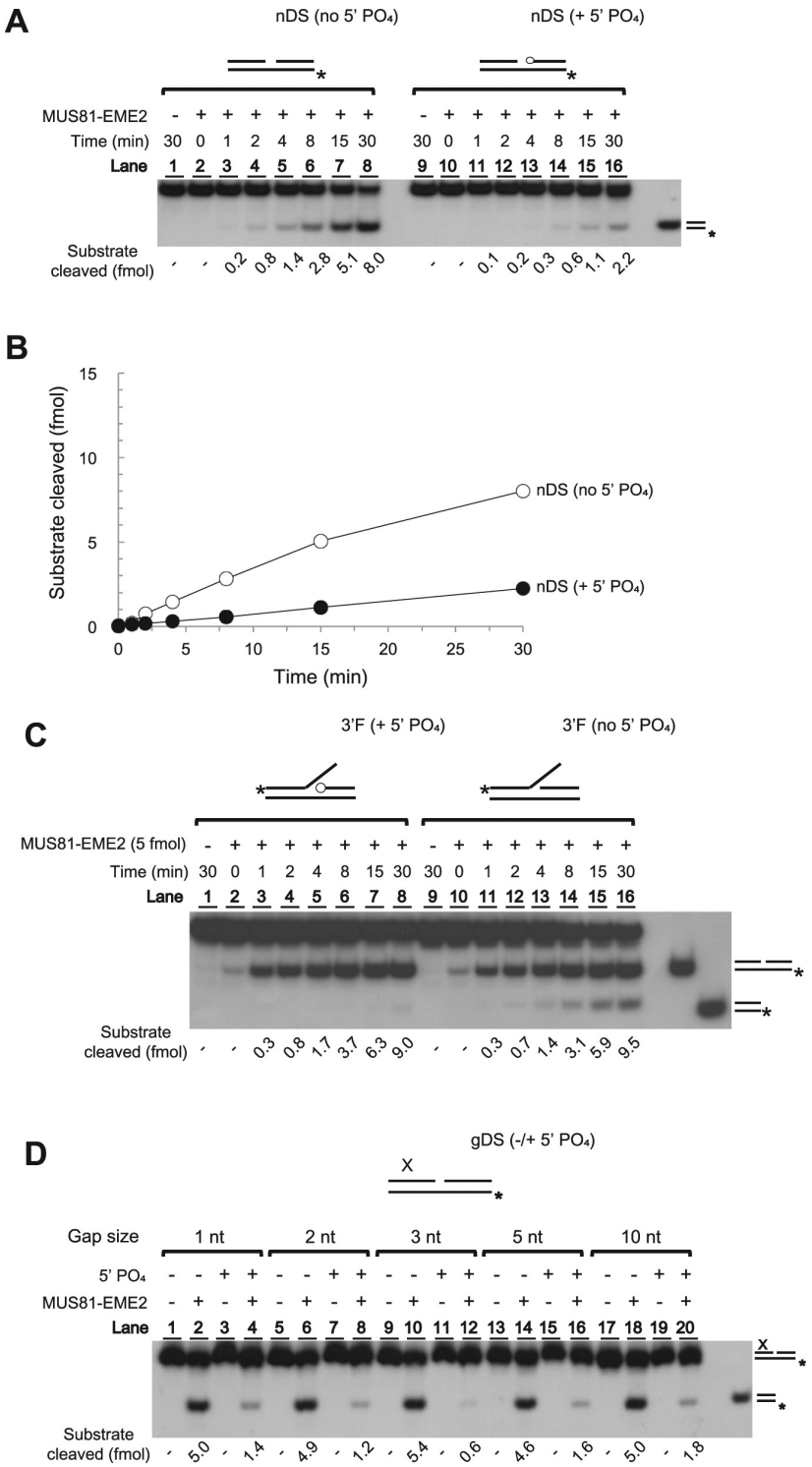

Figure 5. The presence or absence of 5′ phosphate at a nick influences the cleavage of duplex DNA by MUS81-EME2. (**A**) Endonuclease assays were performed using 15 fmol of unligatable (no phopshpate residue at the nick) or ligatable (+5′ phosphate at the nick) nDS and 30 fmol of MUS81-EME2. The structures of DNA substrates are shown at the top of the gel. An open circle indicates a phosphoryl group. Reactions were stopped at the indicated time points (1, 2, 4, 8, 15 and 30 min). (**B**) The amount of cleavage products formed in panel (A) was plotted against incubation time. (**C**) The same reaction as in panel (A) was repeated with 15 fmol of 3′F with and without a phosphoryl group at the 5′ end at the nick of junction. The structures of DNA substrates used are shown at the top of the gel. An open circle indicates a phosphoryl group. (**D**) Endonuclease assays were performed using a fixed amount (30 fmol) of MUS81-EME2 and 15 fmol of gapped duplexes (gDS) of varying length (1–10 nt) of gap, with or without a 5′ phosphate at the 5′ end of the downstream oligonucleotide. The structure of the gDS substrate is shown at the top of the gel. X indicates the upstream strand of varying size. The gap size of each substrate used is as indicated. Addition or omission of MUS81-EME2 and the 5′ phosphoryl group (5′ PO_4) are indicated by '+' or '−', respectively. The marker DNA (25-bp linear duplex) is shown at the right side of the gel. The amount of cleavage products formed is indicated at the bottom of the gel. Asterisks indicate the position of the 5′-^{32}P label.

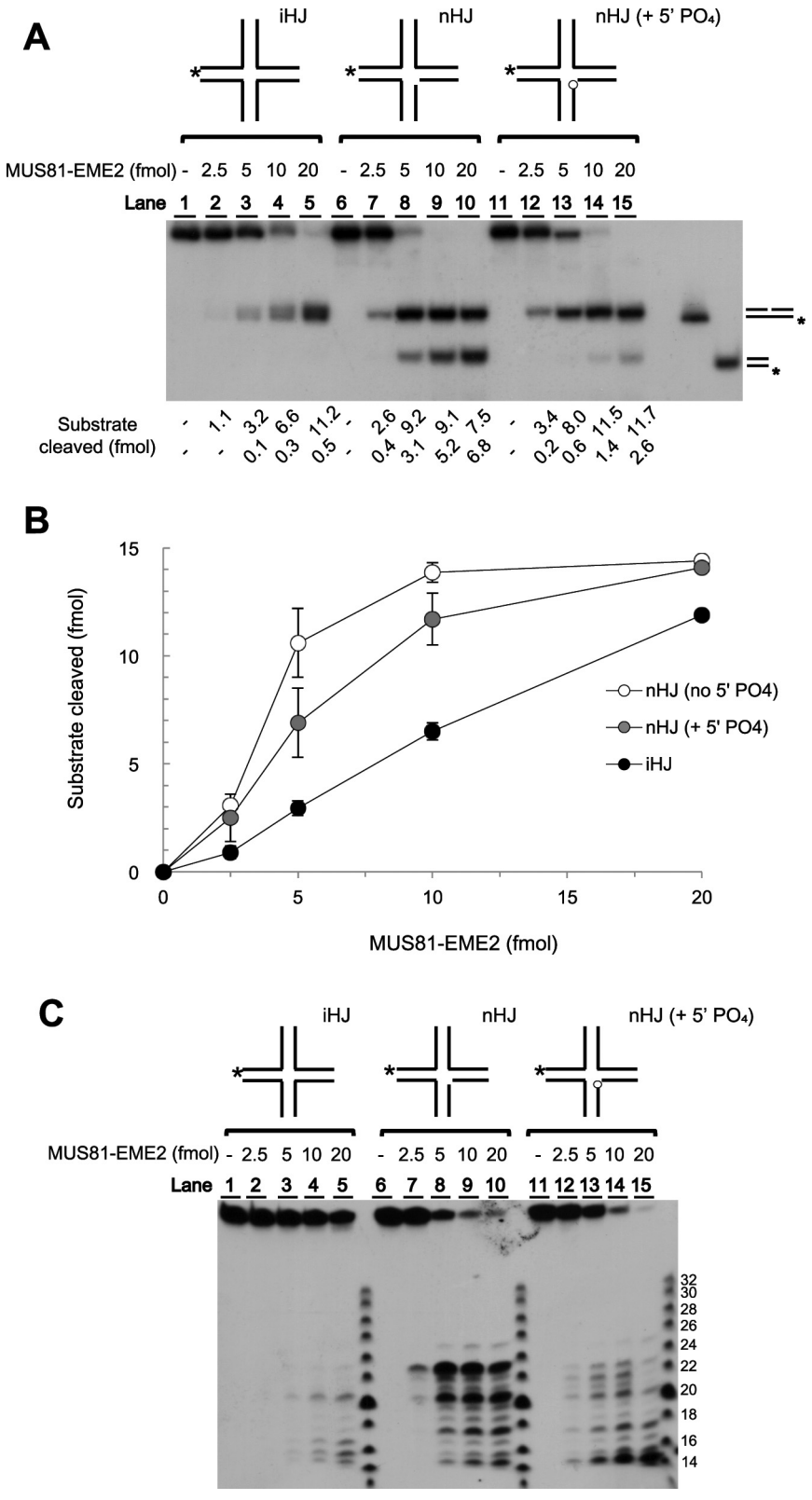

Figure 6. Analysis of HJ cleavage activity of recombinant MUS81-EME2. (**A**) The structures of DNA substrates used are shown at the top of the gel. An open circle indicates a phosphoryl group. Three substrates including iHJ, nHJ (no 5′ PO_4) and nHJ (+5′ PO_4) (15 fmol each) were incubated with increasing amounts (2.5, 5, 10 and 20 fmol) of MUS81-EME2 and the products analyzed as above. Marker DNAs are shown at the right side of the gel. Asterisks indicate the position of the 5′-^{32}**P** label. The amount of cleavage products is indicated at the bottom of the gel. (**B**) The amount of cleavage products formed in panel (A) was plotted against the amount of MUS81-EME2 added. (**C**) The same reactions as in panel (B) were repeated and products were subjected to 15% denaturing PAGE. The molecular mass markers are as described above. Omission of MUS81-EME2 is indicated by '−'.

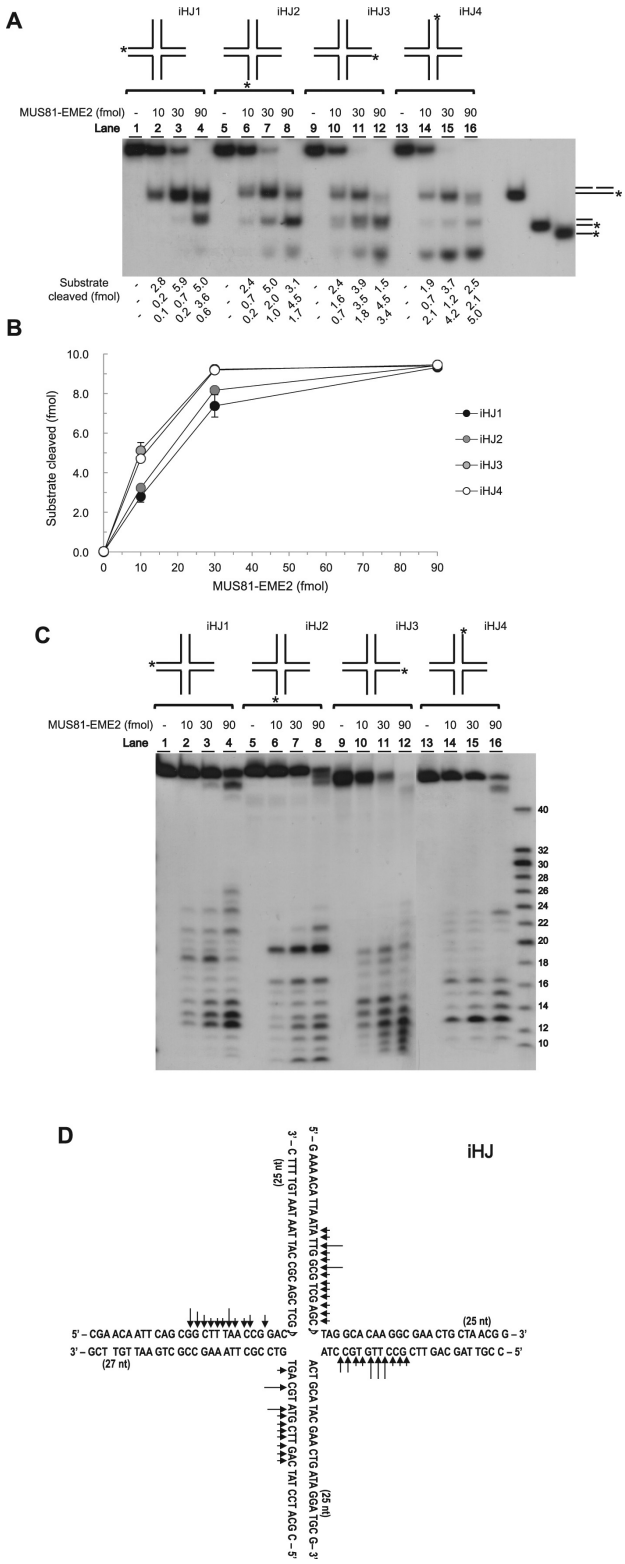

Figure 7. Cleavage sites of human MUS81-EME2 on iHJ. (**A**) Endonuclease assays were performed as described in the Materials and Methods section using four differently labeled iHJ substrates (iHJ1, iHJ2, iHJ3 and iHJ4). Reaction mixtures containing 10 fmol of each iHJ substrate and increasing amounts (10, 30 and 90 fmol) of MUS81-EME2 were incubated for 60 min at 37°C. DNA substrates used are shown at the top of the gel. The three marker DNAs (2-nt gapped 50-bp linear duplex, 25-bp linear duplex and 25-nt ssDNA) are shown at the right side of the gel. Asterisks indicate the position of the 5′-^{32}P label. The amount of cleavage products is indicated at the bottom of the gel. (**B**) The amount of cleavage products formed in panel (A) was plotted against the amount of MUS81-EME2 added. (**C**) The products were subjected to 15% denaturing PAGE. The molecular mass markers are synthetic oligonucleotides labeled at their 5′ ends, and size (nt) is indicated. (**D**) The sites on the iHJ substrate cleaved by MUS81-EME2 are indicated by arrows. Longer arrows indicate preferred cleavage sites.

Table 2. Kinetic parameters for MUS81-EME2 endonuclease activity[a]

Substrate used	V_{max} (nM min^{-1})	K_M (nM)	k_{cat} (min^{-1})	k_{cat}/K_M (nM^{-1} min^{-1})
3′F	2.12 ± 0.29	1.02 ± 0.59	21.24 ± 1.18	20.78 ± 0.03
iHJ	1.12 ± 0.11	0.52 ± 0.06	2.24 ± 0.12	4.31 ± 0.80

[a]Endonuclease assays were performed using varying amounts (5, 10, 20 and 40 fmol) of each substrate and a fixed amount (2 fmol with 3′F and 10 fmol with iHJ) of MUS81-EME2. A master mix (200 μl) for each level of substrate was assembled on ice and reaction was initiated by the addition of 1-mM $MgCl_2$ (final concentration), followed by incubation at 37°C. An aliquot (20 μl) was withdrawn to a tube containing 4 μl of a 6X stop solution at indicated time points (0, 1, 2, 4 and 8 min). The inverse initial velocity ($1/V_0$) was plotted against the inverse of the substrate concentration ($1/[S]$), and the values of K_M and V_{max} were calculated by nonlinear regression. The values were obtained by determining initial rates of cleavage of varying concentrations of the 3′F and iHJ substrates by MUS81-EME2 and represent mean standard deviations of three independent experiments.

Table 3. Optimal concentrations of salts and divalent metal ions for MUS81-EME2

Substrate	Additions or omissions	Concentration (mM, final)	Substrate cleaved (%)
3′F	Complete[a]		100**
	Complete + NaCl	50, 100	290, 91
	Complete + omit $MgCl_2$		<1
	Omit $MgCl_2$ + $MnCl_2$	0.25, 1	114, 85
	Omit $MgCl_2$ + $CaCl_2$	0.25, 1	<1
	Omit $MgCl_2$ + $ZnCl_2$	0.25, 1	<1
	Omit $MgCl_2$ + $CoCl_2$	0.25, 1	67, 7
iHJ	Complete		100***
	Complete + NaCl	50, 100	80, 7
	Complete + KCl	20, 70	112, 30
	Complete + CH_3COONa	20, 70	126, 50
	Complete + omit $MgCl_2$		<1
	Omit $MgCl_2$ + $MnCl_2$	0.25, 1	105, 75
	Omit $MgCl_2$ + $CaCl_2$	0.25, 1	<1
	Omit $MgCl_2$ + $ZnCl_2$	0.25, 1	<1
	Omit $MgCl_2$ + $CoCl_2$	0.25, 1	38, <1

[a]Complete reactions contained 25-mM Tris-HCl/pH8.0, 1-mM $MgCl_2$, 30-mM NaCl and 15 fmol of 3′F or iHJ substrates in the presence of 4 or 20 fmol, respectively, of the recombinant MUS81-EME2 enzyme, followed by incubation at 37°C for 30 min. The amount of each substrate cleaved in the complete reaction was 3.4** and 5.8 fmol***, respectively, with the 3′F and iHJ substrate.

the nDS substrate, being cleaved only by MUS81-EME2 (Figure 2C). No cleavage products were formed by MUS81-EME1. Even higher levels (∼100 fmol) of protein failed to yield cleavage products from nDS substrate (data not shown).

Similar experiments were carried out using an iHJ substrate (15 fmol) that was incubated with two different levels (20 and 40 fmol) of the MUS81 complexes. Under these conditions, only MUS81-EME2 cleaved iHJ, while no cleavage products were detected with MUS81-EME1 (Figure 2D). We noted that formation of second cleavage products with the iHJ substrate was significantly lower than that produced with the 3′F substrate. This difference could be attributed to the fact that the gDS products, the first cleavage products formed from iHJ substrates, differ from those produced from synthetic nDS or gDS DNA substrates (see below); they are a non-ligatable mixture of a gapped DNA duplex with short 5′-flap single-stranded DNA (ssDNA), in which the size of the gap and 5′ flap varies [data not shown (31)].

MUS81-EME2 resolves regressed RFs

We also examined whether recombinant human MUS81-EME1 and MUS81-EME2 cleaved RFs or related structures, including lagging strand regressed RFs (Rla) and leading strand regressed RFs (Rle). For this purpose, three different RF model substrates were prepared and each substrate (15 fmol each) was incubated with increasing amounts (5, 10 and 20 fmol) of the human MUS81 complexes (Figure 3A). In this experiment, the 3′F substrate

was used as a positive control (Figure 3A, lanes 1–7). Both MUS81-EME1 and MUS81-EME2 cleaved RF and Rle substrates with efficiencies similar to those observed with the 3′F substrate: as expected, MUS81-EME2 cleaved the 3′F, RF and Rle substrates more efficiently (3–4-fold) than MUS81-EME1 (Figure 3A, lanes 1–21) and produced both gapped-linear and short-linear duplexes (Figure 3A, lanes 5–7, 12–14 and 19–21). MUS81-EME1 cleaved the Rla substrate poorly (<15% compared to Rle) (Figure 3A, lanes 23–25); in contrast, MUS81-EME2 cleaved this substrate relatively efficiently (Figure 3A, lanes 26–28). The cleavage of Rla by MUS81-EME2 was surprising since it lacked a 5′ end near the junction. It was previously shown that MUS81-catalyzed junction cleavage is directed by the presence of a 5′ end at or near junctions in substrates (25). However, more careful quantitative analyses revealed that the relative locations of 5′ ends with respect to the 3′F did not alter the cleavage site selection in the 3′F substrates, although they affected cleavage efficiency to some extents (34).

We examined this unexpected activity in more detail and compared the cleavages of Rla and Rle substrates by MUS81-EME2. Two differently labeled Rla and Rle substrates (Rla1/Rla2 and Rle1/Rle2), as shown in Figure 3B, were prepared; we found that all four substrates were similarly cleaved by MUS81-EME2. Like the results described above (Figure 3A, lanes 26–28), MUS81-EME2 cleaved both Rla1 and Rla2 and yielded two species of products: a major fast-migrating 5′-overhanged partial duplex and one that was slow migrating in a diffusive way (Figure 3B, lanes 1–8). Analyses of cleavage products using high-resolution gel electrophoresis revealed that the cleavage occurred in only one strand (Figure 3C, lanes 1–4). MUS81-EME2 cleaved the fully duplexed-labeled strand in Rla1 predominantly at one site close to the junction (Figure 3B, lanes 1–2; indicated by an arrow in Figure 3B), but not the labeled strand containing a 5′-free ssDNA (Figure 3C, lanes 3–4). In contrast, cleavage of both Rle1 and Rle2 substrates yielded two distinct products: a gDS and a short linear duplex (Figure 3B, lanes 9–16). In Rle1, the first cleavage occurred over a broad region of the duplex arm (indicated by a solid arrow in Figure 3B, lanes 9–12; Figure 3C, lanes 5–6), while the second cleavage (indicated by an open arrow in Figure 3B) occurred close to the junction (Figure 3C, lanes 7–8). These data indicate that MUS81-EME2 can process a variety of branched structures, suggesting that MUS81-EME2 can play versatile roles in DNA transactions, which need to be clarified in the future.

MUS81-EME2 cleaves two strands among three strands present in an nDS

As described above, we detected significantly lower levels of the second cleavage products formed from iHJ by MUS81-EME2 compared to those obtained from 3′F (compare Figure 1C and D) or nDS/gDS substrates (data not shown; see below). Although the first product formed from iHJ or 3′F is similar to synthetic nDS or gDS substrates in structure, they could differ from each other with regard to a phosphoryl group at the 5′ end at the nick or gap. To address this, we analyzed the pattern of cleavage of synthetic nDS substrates by MUS81-EME2. Three substrates (nDS1, nDS2 and nDS3) were prepared that differed in the position of a ^{32}P-label at the three 5′ ends present in nDS (Figure 4A). We incubated each substrate with increasing amounts of enzyme and analyzed the products formed using a 15% denaturing gel (Figure 4A). This revealed the following: (i) the cleavage detected in the upstream strand occurred primarily near the nick and proceeded in the 3′ to 5′ direction in the presence of increasing amounts of enzyme (Figure 4A, lanes 1–5), resulted in large gaps. The major sites cleaved by MUS81-EME2 in the upstream strand are indicated in Figure 4B. This cleavage pattern is similarly observed with the budding and fission yeast Mus81 complexes, which can produce large gaps with nicked DNA substrates (10,25). (ii) The downstream strand, however, was hardly cleaved (Figure 4A, lanes 6–10). (iii) The template strand was cleaved at three major sites near the nick (Figure 4A, lanes 11–15, 1- to 3-nt away from the nick as shown in Figure 4B). This activity appears unique to human MUS81-EME2 and indicates that it can generate DSBs from nDS substrates.

MUS81-EME2 preferentially cleaves nDSs lacking a 5′ phosphate at the nick

We examined the influence of a 5′ phosphate on the cleavage at the template strand by MUS81-EME2. Two nDS substrates were prepared that were labeled at the 5′ end of the template strand, but differed only in the presence or absence of a phosphoryl group at the 5′ end of the downstream oligonucleotides (Figure 5A). Time–course experiments revealed that MUS81-EME2 cleaved the nDS substrate lacking a 5′ phosphate residue at the nick more efficiently (∼5-fold) than the one containing a 5′ phosphate (Figure 5A, compare lanes 1–8 and 9–16; Figure 5B). We also analyzed the cleavage products and found that the presence of the 5′ phosphate at the nick did not alter the cleavage pattern of the template strand (data not shown). We also examined whether the position of the phosphate in the nick affected template strand cleavage using an nDS substrate containing a phosphoryl group at the 3′ end of the upstream strand. When the same experiment as described in Figure 5A was carried out, rates of cleavage of the two substrates were nearly identical (data not shown). These results indicate that MUS81-EME2 recognizes and is influenced by the 5′ phosphate of the downstream strand, but not by the 3′ phosphate of the upstream strand. This result further indicates that the presence and location of a phosphate in the nick affects markedly the cleavage of the template strand.

Since it was known that the cleavage of 3′F substrate by MUS81 complexes is driven by a 5′ end at or near junction (25), we investigated whether the presence of a phosphoryl group at the 5′ end of the junction could affect the cleavage efficiency. Two 3′F substrates, one with a 5′ phosphate in the downstream strand (Figure 5C, lanes 1–8) and the other devoid of a 5′ phosphate, were prepared (Figure 5C, lanes 9–16). As shown, cleavage of the 3′F strand was not affected by the presence of a phosphate group at the junction; the total level of cleavage products formed with these substrates was almost comparable (Figure 5C). However, short duplex DNA products (the second product) were more efficiently produced from the 3′F substrate lacking a

5′ phosphate (Figure 5C, compare lanes 1–8 and 9–16), indicating that the absence or presence and the relative position of a phosphoryl group at a nick could affect the cleavage of gDS DNA by MUS81-EME2. In order to confirm this and evaluate the influence of the gap size on template strand cleavage, two sets of gDS substrates containing increasing sizes of gaps (1–10 nt) with or without a phosphate at the 5′ end of the downstream strand were prepared (Figure 5D). Gap sizes were adjusted by changing the length of the upstream oligonucleotide (indicated as X in Figure 5D). All substrates tested contained the same downstream and template strands. When each of the gDS substrates (15 fmol) and MUS81-EME2 (30 fmol) were incubated for 30 min at 37°C, substrates lacking a 5′ phosphate residue at the 5′ end of the downstream strand were cleaved more efficiently than those with a 5′ phosphate regardless of the gap size (Figure 5D). Approximately, 1/3 and 1/10 of all gDS substrates were cleaved in the absence and presence, respectively, of a 5′ phosphate (Figure 5D). This result indicates that it is the presence of a 5′ phosphate residue, not the gap size, that influences the cleavage of gDS DNA.

MUS81-EME2 cleaves a variety of HJ substrates

It was shown previously using the *S. pombe* Mus81–Eme1 complex that the presence of a 5′ phosphate at the nick of the junction in nHJ affected cleavage site selection, but not cleavage efficiency (35). In order to investigate whether the 5′ phosphate at the nick affected the human recombinant MUS81-EME2 cleavage activity, three different HJ derivatives were prepared: iHJ and two types of nHJs (one with and the other without a 5′ phosphate at the nick; Figure 6A). We compared the efficiency of cleavage of these three substrates by incubating each substrate (15 fmol) with increasing levels (2.5–20 fmol) of unmodified MUS81-EME2. In keeping with our previous results, MUS81-EME2 cleaved nHJ more efficiently (2–4-fold) than iHJ (Figure 6A, compare lanes 1–5 and 6–15; Figure 6B). MUS81-EME2 cleaved both types of nHJs with comparable efficiency (Figure 6A, compare lanes 6–10 and 11–15), in accord with the previous finding (35). However, we noted a marked difference in the type of products formed from the two nHJ substrates (Figure 6A, compare lanes 6–10 and 10–15), although the total amount of cleavage products formed remained relatively unaffected (Figure 6B, compare open and semi-solid circles). The amount of the second cleavage products (short duplex DNAs) formed from nHJ containing a ligatable nick was significantly lower than that formed from nHJ containing a nick devoid of a 5′ phosphate residue (Figure 6A, lanes 6–10 and 11–15). This is consistent with our finding that MUS81-EME2 cleaves nDS substrates lacking a 5′ phosphate in the nick more efficiently (Figure 5A).

Although the presence of a 5′ phosphate at the nick did not affect the overall cleavage efficiency, it could influence the cleavage site selection as reported (35). We analyzed the cleavage pattern of products derived from each substrate radiolabeled at the 5′ end of the same strand (Figure 6C). This analysis revealed that multiple cleavage products were formed from each substrate; cleavage occurred 1–10-nt distal from the junction point of HJ substrates (Figure 6C). The most significant difference observed was that in the absence of a 5′ phosphate residue, cleavage occurred near the junction point of nHJ with two main cleavage sites (Figure 6C, lanes 7–10). In the presence of a 5′ phosphate residue in the nick, cleavage sites in the labeled strand were detected farther away from the junction toward the arm end, producing predominantly shorter products (Figure 6C, compare lanes 6–10 and 11–15).

Mapping of the cleavage sites on each arm of an iHJ

We found that the presence of a nick and the nature of its end (e.g. ligatable versus unligatable) at the junction in an HJ substrate affected both cleavage efficiency and cleavage site selection (Figure 6). Therefore, we determined the cleavage sites on each arm of the iHJ substrate that lacks a nick altogether. For this purpose, four iHJ substrates (iHJ1, iHJ2, iHJ3 and iHJ4), each with a differently labeled strand, were prepared (Figure 7A). Each substrate (10 fmol) was incubated with three different concentrations (10, 30 and 90 fmol) of MUS81-EME2 and the cleavage products formed were analyzed in native and denaturing gels. As shown in Figure 7B, the total amount of cleavage products formed from each iHJ substrate was similar as expected from the fact that these substrates are identical except for the position of radiolabel. All four iHJ substrates produced three types of products, which varied markedly depending on the labeled strand used (Figure 7A, compare lanes 1–4, 5–8, 9–12 and 13–16). For example, formation of the smallest product was most prominent with iHJ4 (Figure 7A, lanes 13–16), while formation of the gDS product was most efficient with iHJ1 (Figure 7A, lanes 1–4). The fastest-migrating products, especially prominent in lanes 14–16 (Figure 7A), are most likely short ssDNA dissociated from the linear duplex products after the secondary 3′-to-5′ directional degradation of the upstream strand by MUS81-EME2 in keeping with the result shown in Figure 4. This could be attributed to sequence differences in each arm, which affects the cleavage efficiency of each labeled strand. The results obtained using the denaturing gel separation, shown in Figure 7C, support this possibility since the preferred cleavage sites in each strand differed, being located 2–14 nt to the 5′ side of the junction on all four arms (Figure 7C and 7D). Thus, human MUS81-EME2 isolated from *E. coli* cleaves iHJ on the 5′ side near the junction, in keeping with results obtained with other Mus81 complexes (31,36,37).

The regulatory subunit is important for HJ resolvase activity

Previously, it was shown that a truncated recombinant human MUS81–EME1 complex, containing the C-terminal fragments of MUS81 (amino acid 260–551) and EME1 (amino acid 244–571), catalyzed the resolution of iHJ structure into linear duplex products (38). In contrast, the recombinant full-length MUS81–EME1 complex, purified from *E. coli*, was poorly active with the same substrate (20). Since EME1 is larger than EME2, but shares high homology with EME2 at the C-terminus, it is possible that the bulky N-terminal region of EME1 prevents the resolution of iHJ substrates by the MUS81–EME1 complex by imposing a steric hindrance during its binding to iHJ structure. To test

this notion, we prepared human MUS81-EME1(244–583), a mutant MUS81 complex containing a N-terminally truncated EME1 fragment (amino acids 244–583).

The human MUS81-EME1(244–583), MUS81-EME1 and MUS81-EME2 complexes all isolated from *E. coli* were analyzed for their ability to cleave nHJ and iHJ substrates as shown in Figure 8. Incubation of the nHJ substrates with increasing amounts (12, 25 and 50 fmol) of each complex revealed that MUS81-EME2 cleaved nHJ more efficiently than wild-type MUS81-EME1 and MUS81-EME1(244–583) (Figure 8A and B). MUS81-EME1(244–583) and wild-type MUS81-EME1 cleaved the nHJ substrate with nearly identical but lower rates (Figure 8A, lanes 2–4 and 5–7; Figure 8B). In keeping with the result above, MUS81-EME2 cleaved nHJ efficiently (Figure 8A, lanes 8–10). We obtained nearly identical results with 3′F substrates (data not shown). When we tested the iHJ substrate, only MUS81-EME2 cleaved this iHJ substrate (Figure 8C and D). In contrast, MUS81-EME1(244–583) and MUS81-EME1 cleaved iHJ poorly (Figure 8C, lanes 2–4 and 5–7; Figure 8D). These results indicate that truncation of the N-terminal fragment does not influence the cleavage efficiency of the MUS81–EME1 complex and that HJ-resolvase activity of MUS81-EME2 is critically dependent on the EME2 subunit.

DISCUSSION

In this study, we presented experimental data indicating that the human MUS81–EME2 complex possesses two intrinsic enzymatic activities distinct from other known Mus81 complexes including human MUS81-EME1. Unmodified recombinant MUS81-EME2 and MUS81-EME1 isolated from *E. coli* differ from each other in substrate specificity, the former being able to resolve iHJ and nDS/gDS DNA. Previously, it was shown that a recombinant human complex consisting of N-terminally truncated fragments of both MUS81 and EME1 displayed enhanced activity for iHJ substrates compared to the full-length wild-type complex *in vitro*. The cleavage efficiency of this truncated version of MUS81 complex was still much lower with iHJs than with nHJs. However, the nHJ/iHJ-cleavage ratio was significantly increased (∼3-fold) when an immunoprecipitated endogenous complex was used as the enzyme source (38). When we carried out assays with MUS81-EME2 using intact and nHJs as substrates, the nHJ/iHJ-cleavage ratio was ∼3, similar to that obtained with the immunoprecipitated endogenous MUS81 complex. Thus, one interpretation is that the increased activity of MUS81 could be attributed to the MUS81–EME2 complex presence in the immunoprecipitated materials. However, it is equally possible that the robust MUS81 activity observed in the immunoprecipitates was due to the phosphorylated and, hence, activated form of MUS81-EME1 as shown by Dr West and his colleagues using yeast Mus81-Mms4 (39,40). The recent findings by the same group also suggest a third scenario; MUS81-EME1 is associated with SLX1-SLX4, another structure-selective endonuclease at the G2/M transition in response to phosphorylation of EME1 and SLX4, forming a stable SLX-MUS holoenzyme that catalyzes more efficient and coordinated cleavage of HJs (41).

Recently, various forms of human recombinant MUS81–EME1/EME2 complexes from *E. coli* were prepared in order to assess the influence of the winged helix (WH; residues128–250) domain of human MUS81 on the incision activities of the two complexes (42). Differences in reaction conditions (25°C versus 37°C; 90 versus 30 min; 5 versus 1-mM Mg^{2+}) and the amount of enzymes (25 versus 10 fmol) and substrates (90 versus 15 fmol) used have made it difficult to directly compare specific activities of wild-type MUS81–EME1 and MUS81–EME2 complexes from the two laboratories. However, we noted that the cleavage of iHJ observed with MUS81-EME2 by McDonald and his colleagues is not as noticeable as we observed (42). This is most likely due to the higher concentrations of Mg^{2+} used. We found that the cleavage of iHJ is rather inhibited in the presence of higher concentrations (>4 mM) of Mg^{2+} (data not shown). More importantly, the results in this study revealed that the WH domain of MUS81 affected both DNA binding and endonuclease activity of MUS81 (42). Some WH proteins such as HNF-3γ and E2F were shown to bind DNA using a canonical DNA interaction that involved major groove recognition and phosphodiester binding by the structural elements present in the WH domains (43). The highly basic WH domain of human MUS81 contained a recognition helix α3 with several Arg/Lys residues critical for binding near junction in the branch substrates (42). It was shown that the basic residues (R186, R191 in human, K176, K181 in *S. pombe*) of MUS81 were important for this binding (42). We speculate that EME2 in a complex context could affect the conformation of the WH domain of MUS81 so that the side chains of Arg or Lys in the recognition helix α3 can interact with a phosphate group at nicks or gaps in duplex DNA. This could provide an underlying mechanism by which the location and/or the presence of a phosphate group at nicks or gaps affects MUS81-EME2-catalyzed cleavage of nDS or gDS DNA.

Although EME2 was first identified a decade ago (19), there is still no evidence in the literature to support the notion that the protein is expressed in human cells. In order to address this issue, we performed a real-time quantitative reverse transcriptase PCR with several pairs of primers along with a TaqMan® probe unique to each primer pair and found that the *EME2* gene is expressed in HeLa cells at a transcriptional level (data not shown). In humans, EME2 (349 aa), which is much smaller than EME1 (570 aa), shares considerable similarity with the C-terminal region of EME1. One possible explanation for the unique iHJ-cleavage activity of MUS81-EME2 isolated from *E. coli* is that its smaller EME2 subunit may be critical for the complex to efficiently bind/cleave both the relatively inflexible iHJ (including nDS/gDS) and the flexible nHJ structure. The larger EME1 subunit may allow the complex to access only more flexible substrates such as nHJ. As shown in Figure 8, the MUS81 complex containing a truncated EME1 subunit, similar in size to EME2, failed to cleave iHJ as well as nDS/gDS substrates. These findings suggest that the EME2 subunit is essential for iHJ-cleavage activity observed in conjunction with the catalytic MUS81 subunit.

We showed that human MUS81-EME2 has intrinsic HJ resolution activity as well as nicked or gapped linear duplex cleavage activity. Low levels (<20 fmol) of MUS81-

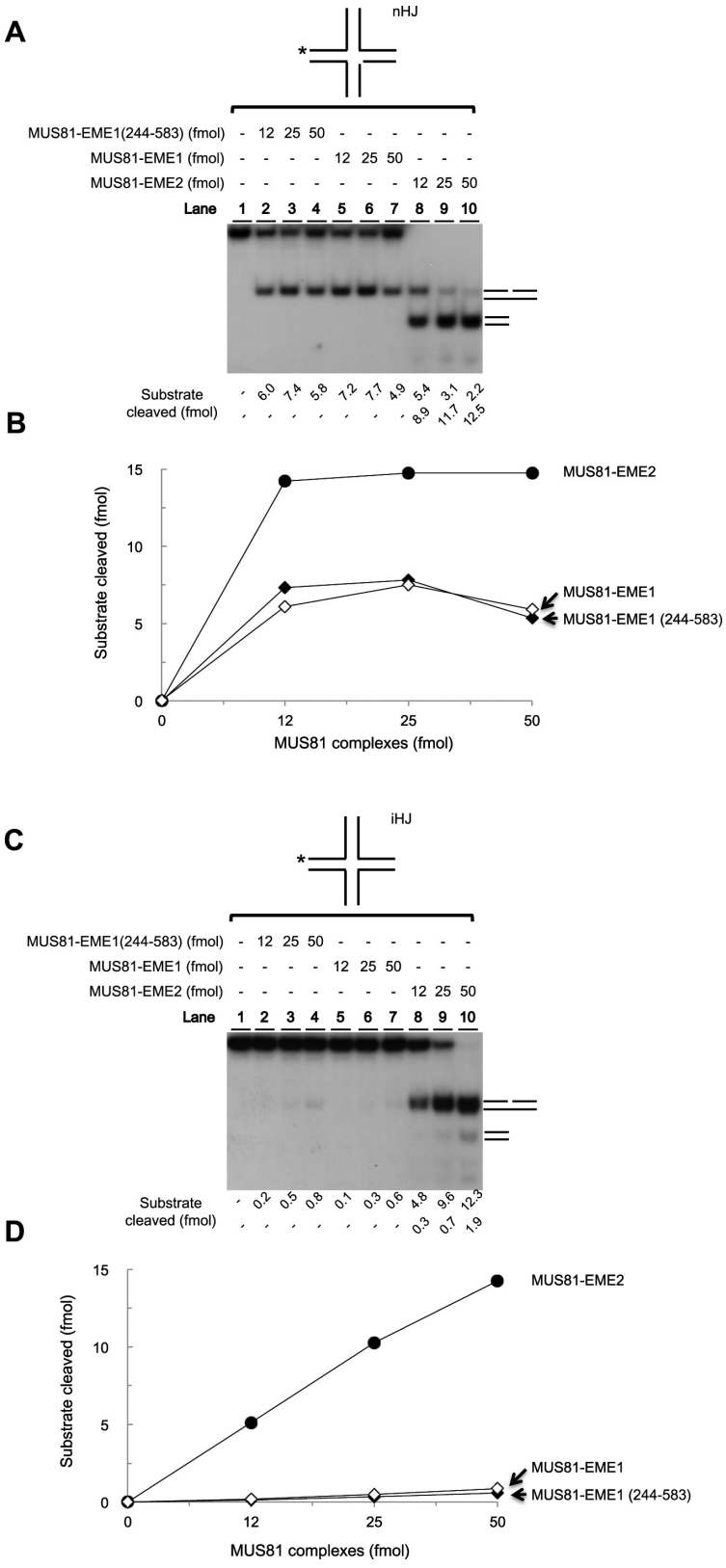

Figure 8. The C-terminal EME1 fragment does not substitute for EME2. Endonuclease assays were performed as described in the Materials and Methods section using nHJ (**A**) and iHJ (**C**) substrates. A fixed amount (15 fmol) of DNA substrate was incubated for 60 min at 37°C with increasing amounts (12, 25 and 50 fmol) of MUS81-EME1(244–583), MUS81-EME1 and MUS81-EME2. DNA substrates used are shown at the top of the gel. The amount of cleavage products is indicated at the bottom of the gel. (**B**) and (**D**) The amount of cleavage products formed in panels (A) and (C), respectively, was plotted against the amount of each MUS81 complex used.

EME2 cleaved iHJ substrates efficiently, whereas high levels (~100 fmol) of MUS81-EME1 cleaved neither the iHJ nor the nDS substrate. The enzymatic properties of the well-studied human recombinant MUS81–EME1 complex are shared with all known recombinant Mus81 complexes, thus being functional orthologs. Our results suggest that MUS81-EME2 in mammalian cells may play a more versatile role than MUS81-EME1 in DNA repair and replication for the following reasons: (i) the specific activity of MUS81-EME2 is significantly higher (>5-fold) than that of MUS81-EME1 (20). (ii) MUS81-EME2 could be more abundant than MUS81-EME1, based on the immunoprecipitated materials obtained in the immnunoprecipitation experiment described above. To confirm this, the relative abundance of the two MUS81 complexes needs to be determined. (iii) Resolution of iHJ or nHJ by MUS81-EME2 produces various products including short 5′ flap, nDS or gDS structures, some of which are substrates that can be converted further into DSB by MUS81-EME2. As described above, the cleavage of an nDS/gDS by MUS81-EME2 was suppressed by the presence of 5′ phosphate at the nick. This type of discontinuity in DNA can be readily repaired by extension, followed by DNA ligation. In keeping with this notion, the cleavage of nDS by MUS81-EME2 was unaffected by the presence of a phosphoryl group at the 3′ end of a nick. Thus, MUS81-EME2 is a more versatile enzyme than MUS81-EME1 and well-suited to process a number of aberrant DNA structures for subsequent repair pathways. (iv) Finally, MUS81-EME2 can process a diverse form of RFs, which is an important property required to rescue stalled or collapsed RFs. MUS81-EME2 cleavage reactions yield 5′ overhang partial duplex products from lagging strand regressed RF (Rla) and a slower migrating product, which is less prominent than the 5′ overhang duplex product on a native gel (Figure 3B). When we analyzed the structure of the slow-migrating products, we found that they were gDS structures with 5′ flaps; such structures were generated by cleavage at the third strand that is fully duplexed with other strands, in keeping with a previous report (10). These data indicate that MUS81-EME2 is suitable to repair stalled and regressed RFs during DNA replication. In support of this notion, it was reported that DSB formation and subsequent recovery of stalled RFs were reduced in Mus81-deficient mouse embryonic stem cells (44).

Previously, it was shown that human MUS81-EME1 prepared from mammalian cells cleaved mobile HJ to limited extents (19,31,45). We also examined whether MUS81-EME2 isolated from *E. coli* cleaved mobile iHJ more efficiently than static iHJ. The mobile HJ substrate differed from the static HJ in that it contained a 10-bp homologous, and thus branch-migratable, region at its junction core. We found no significant difference in cleavage efficiency with MUS81-EME2 (data not shown). This result indicates that MUS81-EME2 isolated from *E. coli* acts in a structure-selective manner and does not depend on a migratable junction. We showed in this study that MUS81-EME2 displayed stronger activities *in vitro* for many types of DNA structures compared to MUS81-EME1; this holds true for recombinant MUS81-EME1/2 complexes purified from *E. coli* that lack any post-translational modifications such as phosphorylation. Recent findings that CDK/PLK1-mediated phosphorylation of MUS81-EME1 activated enzymatic activities, directly or indirectly, via its association with SLX1-SLX4 (41) suggest the possibility that MUS81-EME1 could play a more important role in a certain, not all, aspect of DNA metabolisms than MUS81-EME2. The fact that both human MUS81 complexes share great similarity in enzymatic properties and substrate specificity suggests that MUS81-EME2 appears simply a more active version of MUS81-EME1. Considering that MUS81-EME1 activity is markedly stimulated by phosphorylation, the regulated enhancement of MUS81-EME1 may not be of much use particularly in the presence of a similar enzyme, but with much stronger activity. This rationale is also in keeping with the notion that they may differ at least in spatial and temporal regulation and thus in their physiological function. As human cells have two distinct MUS81 complexes, it would be important to determine the precise physiological roles *in vivo* of each complex in DNA transactions and how these two complexes are regulated. The availability of knock-out mice lacking either EME1 or EME2 may help answer these important questions.

ACKNOWLEDGMENTS

We thank Dr Jerard Hurwitz for critical reading of the manuscript. We also thank Dr Stephen C. West for the kind gift of expression vectors for MUS81 complexes.

FUNDING

Funding for open access charge: National Research Foundation of Korea, Ministry of Education, Science and Technology [2012R1A2A2A01047260].
Conflict of interest statement. None declared.

REFERENCES

1. Kuzminov,A. (1995) Collapse and repair of replication forks in *Escherichia Coli Mol. Microbiol.*, **16**, 373–384.
2. Fabre,F., Chan,A., Heyer,W.D. and Gangloff,S. (2002) Alternate pathways involving Sgs1/Top3, Mus81/Mms4, and Srs2 prevent formation of toxic recombination intermediates from single-stranded gaps created by DNA replication. *Proc. Natl. Acad. Sci. U.S.A.*, **99**, 16887–16892.
3. Cox,M.M., Goodman,M.F., Kreuzer,K.N., Sherratt,D.J., Sandlerk,S.J. and Marians,K.J. (2000) The importance of repairing stalled replication forks. *Nature*, **404**, 37–41.
4. Kowalczykowski,S.C. (2000) Initiation of genetic recombination and recombination-dependent replication. *Trends Biochem. Sci.*, **25**, 156–165.
5. Higgins,N.P., Kato,K. and Strauss,B. (1976) A model for replication repair in mammalian cells. *J. Mol. Biol.*, **101**, 417–425.
6. Seigneu,M., Bidnenko,V., Ehrlich,S.D. and Michel,B. (1998) RuvAB acts at arrested replication forks. *Cell*, **95**, 419–430.
7. Lilley,D.M. and White,M.F. (2001) The junction-resolving enzymes. *Nat. Rev. Mol. Cell Biol.*, **433**, 433–443.
8. Ralf,C., Hickson,I.D. and Wu,L. (2006) The Bloom's syndrome helicase can promote the regression of a model replication fork. *J. Biol. Chem.*, **32**, 22839–22846.
9. Sharples,G.J. (2001) The X philes: structure-specific endonucleases that resolve Holliday junctions. *Mol. Microbiol.*, **39**, 823–834.
10. Gaillard,P.H., Noguchi,E., Shanahan,P. and Russell,P. (2003) The endogenous Mus81-Eme1 complex resolves Holliday junctions by a nick and counternick mechanism. *Mol. Cell*, **12**, 747–759.
11. Takahagi,M., Iwasaki,H. and Shinagawa,H. (1994) Structural requirements of substrate DNA for binding to and cleavage by RuvC, a Holliday junction resolvase. *J. Biol. Chem.*, **269**, 15132–15139.

12. Whitby,M.C. and Dixon,J. (1998) Substrate specificity of the SpCCE1 Holliday junction resolvase of *Schizosaccharomyces pombe*. *J. Biol. Chem.*, **273**, 35063–35073.
13. Ip,S.C.Y., Rass,U., Blanco,M.G., Flynn,H.R., Skehel,J.M. and West,S.C. (2008) Identification of Holliday junction resolvases from humans and yeast. *Nature*, **456**, 357–361.
14. Rass,U., Compton,S.A., Matos,J., Singleton,M.R., Ip,S.C.Y., Blanco,M.G., Griffith,J.D. and West,S.C. (2010) Mechanism of Holliday junction resolution by the human GEN1 protein. *Genes Dev.*, **24**, 1559–1569.
15. Fekairi,S., Scaglione,S., Chahwan,C., Taylor,E.R., Tissier,A., Coulon,S., Dong,M.Q., Ruse,C., Yates,J.R. III, Russell,P. *et al.* (2009) Human SLX4 is a Holliday junction resolvase subunit that binds multiple DNA repair/recombination endonucleases. *Cell*, **138**, 78–89.
16. Svendsen,J.M., Smogorzewska,A., Sowa,M.E., O'Connell,B.C., Gygi,S.P., Elledge,S.J. and Harper,J.W. (2009) Mammalian BTBD12/SLX4 assembles a Holliday junction resolvase and is required for DNA repair. *Cell*, **138**, 63–77.
17. Andersen,S.L., Bergstralh,D.T., Kohl,K.P., LaRocque,J.R., Moore,C.B. and Sekelsky,J. (2009) Drosophila MUS312 and the vertebrate ortholog BTBD12 interact with DNA structure-specific endonucleases in DNA repair and recombination. *Mol. Cell*, **35**, 128–135.
18. Ciccia,A., McDonald,N. and West,S.C. (2008) Structural and functional relationships of the XPF/MUS81 family of proteins. *Annu. Rev. Biochem.*, **77**, 259–287.
19. Ciccia,A., Constantinou,A. and West,S.C. (2003) Identification and characterization of the human Mus81/Eme1 endonuclease. *J. Biol. Chem.*, **278**, 25172–25178.
20. Ciccia,A., Ling,C., Coulthard,R., Yan,Z., Xue,Y., Meetei,A.R., Laghmani,E.H., Joenje,H., McDonald,N., de Winter,J.P. *et al.* (2007) Identification of FAAP24, a Fanconi Anemia core complex protein that interacts with FANCM. *Mol. Cell*, **25**, 331–343.
21. Wu,L. and Hickson,I.D. (2003) The Bloom's syndrome helicase suppresses crossing over during homologous recombination. *Nature*, **426**, 870–874.
22. Boddy,M.N., Lopez-Girona,A., Shanahan,P., Interthal,H., Heyer,W.D. and Russell,P. (2000) Damage tolerance protein mus81 associates with the FHA1 domain of checkpoint kinase cds1. *Mol. Cell. Biol.*, **20**, 8758–8766.
23. Interthal,H. and Heyer,W.D. (2000) *MUS81* encodes a novel helix–hairpin–helix protein involved in the response to UV- and methylation-induced DNA damage in *Saccharomyces cerevisiae*. *Mol. Gen. Genet.*, **263**, 812–827.
24. Doe,C.L., Ahn,J.S., Dixon,J. and Whitby,M.C. (2002) Mus81–Eme1 and Rqh1 involvement in processing stalled and collapsed replication forks. *J. Biol. Chem.*, **277**, 32753–32759.
25. Bastin-Shanower,S.A., Fricke,W.M., Mullen,J.R. and Brill,S.J. (2003) The mechanism of Mus81-Mms4 cleavage site selection distinguishes it from the homologous endonuclease Rad1-Rad10. *Mol. Cell. Biol.*, **23**, 3487–3496.
26. Gao,H., Chen,X.B. and McGowan,C.H. (2003) Mus81 endonuclease localizes to nucleoli and to regions of DNA damage in human S-phase cells. *Mol. Biol. Cell*, **14**, 4826–4834.
27. Hollingsworth,N.M. and Brill,S.J. (2004) The Mus81 solution to resolution: generating meiotic crossovers without Holliday junctions. *Genes Dev.*, **18**, 117–125.
28. Kaliraman,V., Mullen,J.R., Fricke,W.M., Bastin-Shanower,S.A. and Brill,S.J. (2001) Functional overlap between Sgs1-Top3 and the Mms4-Mus81 endonuclease. *Genes Dev.*, **15**, 2730–2740.
29. Kang,M.J., Lee,C.H., Kang,Y.H., Cho,I.T., Nguyen,T.A. and Seo,Y.S. (2010) Genetic and functional interactions between Mus81-Mms4 and Rad27. *Nucleic Acids Res.*, **38**, 7611–7625.
30. Ehmsen,K.T. and Heyer,W.D. (2008) *Saccharomyces cerevisiae* Mus81-Mms4 is a catalytic, DNA structure-selective endonuclease. *Nucleic Acids Res.*, **36**, 2182–2195.
31. Chen,X.B., Melchionna,R., Denis,C.M., Gaillard,P.H., Blasina,A., Van de Weyer,I., Boddy,M.N., Russell,P., Vialard,J. and McGowan,C.H. (2001) Human Mus81-associated endonuclease cleaves Holliday junctions *in vitro*. *Mol. Cell*, **8**, 1117–1127.
32. Shin,Y.K., Amangyeld,T., Nguyen,T.A., Munashingha,P.R. and Seo,Y.S. (2012) Human MUS81 complexes stimulate flap endonuclease 1. *FEBS J.*, **279**, 2412–2430.
33. Geuting,V., Kobbe,D., Hartung,F., Durr,J., Focke,M. and Puchta,H. (2009) Two distinct MUS81-EME1 complexes from Arabidopsis process Holliday Junctions. *Plant Physiol.*, **150**, 1062–1071.
34. Ehmsen,K.T. and Heyer,W.D., (2009) A junction branch point adjacent to a DNA backbone nick directs substrate cleavage by *Saccharomyces cerevisiae* Mus81-Mms4. *Nucleic Acids Res.*, **37**, 2026–2036.
35. Osman,F., Gaskell,L. and Whitby,M.C. (2009) Efficient second strand cleavage during Holliday junction resolution by RuvC requires both increased junction flexibility and an exposed 5' phosphate. *PLoS ONE*, **4**, e5347.
36. Boddy,M.N., Pierre-Henri,L., Gaillard,McDonald, W.H., Shanahan,P., Yates,J.R. and Russell,P. (2001) Mus81-Eme1 are essential components of a Holliday Junction Resolvase. *Cell*, **107**, 537–548.
37. Gaskell,L.J., Osman,F., Gilbert,R.J. and Whitby,M.C. (2007) Mus81 cleavage of Holliday junctions: a failsafe for processing meiotic recombination intermediates? *EMBO J.*, **26**, 1891–1901.
38. Taylor,E.R. and McGowan,C.H. (2008) Cleavage mechanism of human Mus81-Eme1 acting on Holliday-junction structures. *Proc. Natl. Acad. Sci. U.S.A.*, **105**, 3757–3762.
39. Matos,J., Blanco,M.G., Maslen,S., Skehel,J.M. and West,S.C. (2011) Regulatory control of the resolution of DNA recombination intermediates during meiosis and mitosis. *Cell*, **147**, 158–172.
40. Matos,J., Blanco,M.J. and West,S.C. (2013) Cell-cycle kinases coordinate the resolution of recombination intermediates with chromosome segregation. *Cell Rep.*, **4**, 78–86.
41. Wyatt,H.D.M., Sarbajna,S., Matos,J. and West,S.C. (2013) Coordinated actions of SLX1-SLX4 and MUS81-EME1 for Holliday junction resolution in human cells. *Mol. Cell*, **52**, 234–247.
42. ,A.J., Schalbetter,S., Bowles,M., Harris,R., Lally,J., Carr,A.M. and McDonald,N.Q. (2013) A winged helix domain in human MUS81 binds DNA and modulates the endonuclease activity of MUS81 compelxes. *Nucleic Acids Res.*, **41**, 9741–9752.
43. White,A., Ding,X., vanderSpek,J.C., Murphy,J.R. and Ringe,D. (1998) Structure of the metal-ion-activated diphtheria toxin repressor/tox operator complex. *Nature*, **394**, 502–506.
44. Hanada,K., Budzowska,M., Davies,S.L., Drunen,E.V., Onizawa,H., Beverloo,H.B., Mass,A., Essers,J., Hickson,I.D. and Kanaar,R. (2007) The structure-specific endonuclease Mus81 contributes to replication restart by generating double-strand DNA breaks. *Nature*, **14**, 1096–1104.
45. Constantinou,A., Chen,X.B., McGowan,C.H. and West,S.C. (2002) Holliday junction resolution in human cells: two junction endonucleases with distinct substrate specificities. *EMBO J.*, **21**, 5577–5585.